

# Amphiphilic Block Copolymer Templated Synthesis of Mesoporous Indium Oxides with Nanosheet-Assembled Pore walls

Yuan Ren<sup>†</sup>, Xinran Zhou<sup>†</sup>, Wei Luo<sup>‡</sup>, Pengcheng Xu<sup>ψ</sup>, Yongheng Zhu<sup>†,§</sup>, Xinxin Li<sup>ψ</sup>, Xiaowei Cheng<sup>†</sup>, Yonghui Deng<sup>\*†,ψ</sup>, Dongyuan Zhao<sup>†</sup>

<sup>†</sup> Department of Chemistry, State Key Laboratory of Molecular Engineering of Polymers, Shanghai Key Laboratory of Molecular Catalysis and Innovative Materials, iChEM (Collaborative Innovation Center of Chemistry for Energy Materials), Fudan University, Shanghai 200433, China

<sup>‡</sup> College of Materials Science and Engineering, Donghua University, Shanghai 201620, China

<sup>§</sup> College of Food Science and Technology, Shanghai Ocean University, Shanghai 201306, China

<sup>ψ</sup> State Key Lab of Transducer Technology, Shanghai Institute of Microsystem and Information Technology, Chinese Academy of Sciences, Shanghai 200050, China

Email: yhdeng@fudan.edu.cn

## Experimental details for micro-sensor fabrication and sensing performance measurement

**Chip fabrication :** In the clean room, micro-hotplate chips (Figure 5a,b) can be low-cost fabricated in batches by using micro-electro-mechanical-systems (MEMS) technologies. The chips were fabricated on a normal single-side polished silicon wafer. In order to improve the accuracy of working-temperature and reduce the power consumption, suspended structure of the micro-hotplate was designed. In the fabricated micro-hotplate chips, four functional components including comb-finger electrodes, poly-Si heater, insulating layer and suspended plate were integrated. With the FEM analysis tool COMSOL, thermal simulation was implemented to validate the design of the micro-hotplate. Besides thermal simulation, the temperature coefficient of resistance of the Poly-Si heater is further calibrated in a temperature programmable oven. Based on the linear fitting relationship between temperature versus heating voltage, the working temperature on sensing area of the micro-hotplate can be well controlled by adjusting the voltage supply.

**Sensor preparation:** 0.01 g of the mesoporous  $\text{In}_2\text{O}_3$  sample was added into 1.0 mL of deionized water and dispersed under ultrasonic to form a crude suspension. After that, 1.0  $\mu\text{L}$  of the suspension was loaded onto the sensing area (i.e. comb-like electrode) of the micro-hotplate chip to form a chemiresistor-type microsensor. Then, the microsensor was dried in an oven at 80  $^{\circ}\text{C}$  for about 2 h (Figure S9). The sensing response was defined as the resistance change of  $\Delta R = R_{\text{NO}_2}/R_0$ . The working temperature of the sensor was induced by a voltage adjustable DC power source, which was connected to the micro-heater. The resistance of the microsensor was real-time recorded by using a commercial multimeter (model: Agilent-34410A). The gas sensing tests were carried out in a lab-made testing chamber (20 L in volume), where the microsensor was previously put inside. In order to obtain  $\text{NO}_2$  with a desired concentration, the standard  $\text{NO}_2$  gas with known volume was injected into the testing chamber and, thereafter, rapidly diluted by ambient air. When  $\text{NO}_2$  gas was introduced to the testing chamber, the  $\text{NO}_2$  molecules adsorbed by the mesoporous  $\text{In}_2\text{O}_3$  will capture electrons from the material that can be detected by the signal of resistance increase. After each test for a concentration, the cover of the testing chamber was removed and the atmosphere of the testing chamber was switched to fresh air for signal recovery. Under fresh air, the  $\text{NO}_2$  molecules desorbed from the mesoporous  $\text{In}_2\text{O}_3$  and released the captured electrons. The released electrons made the resistance of the mesoporous  $\text{In}_2\text{O}_3$  decreased.

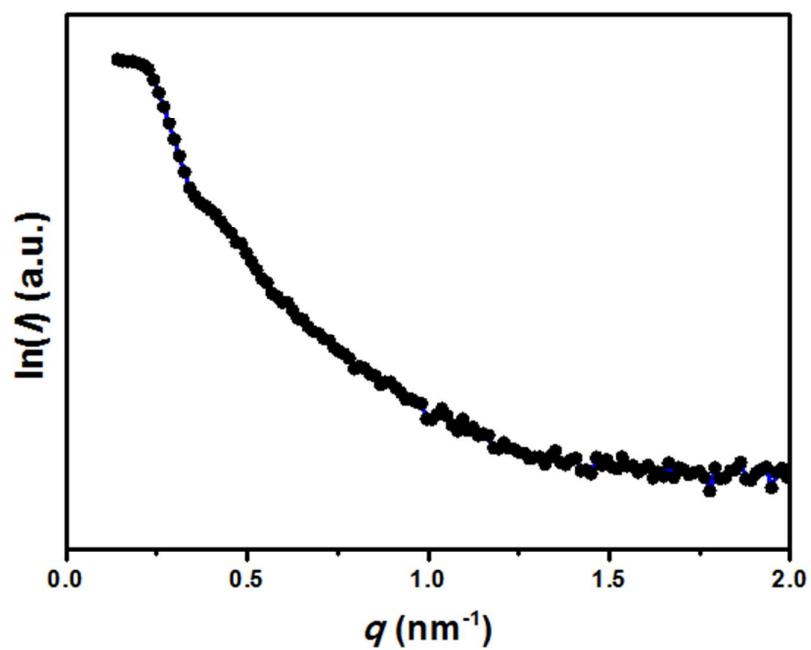


**Figure S1.** SAXS patterns of the as-made PEO-*b*-PS/ $\text{In}_2\text{O}_3$  hybrid sample with a weight ratio (PEO-*b*-PS:  $\text{In}_2\text{O}_3$ ) of 3.0.

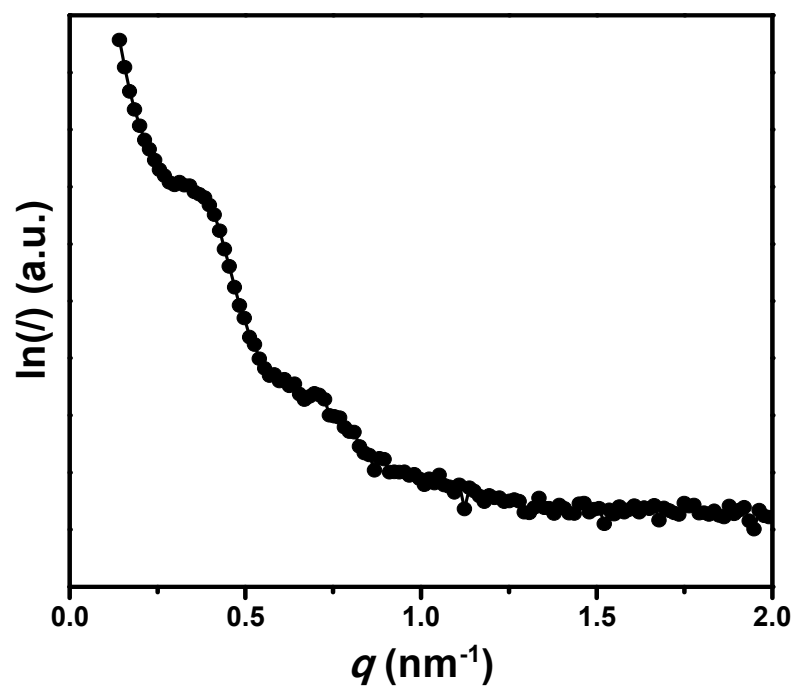


**Figure S2.** SAXS patterns of the  $\text{In}_2\text{O}_3$ -2.5-400-0.5 sample obtained after calcination of the as-made organic-inorganic composite with a weight ratio ( $\text{InCl}_3$ :PEO-*b*-PS) of 2.5 at 400 °C for 0.5h in the presence of comburent  $\text{CaO}_2$  in a muffle furnace.

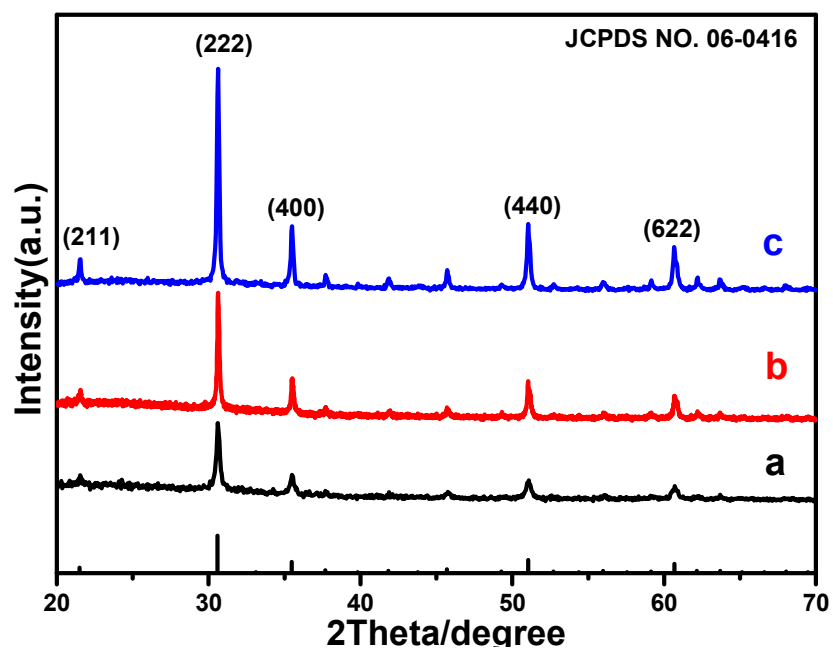


**Figure S3.** Wide angle XRD patterns of the In<sub>2</sub>O<sub>3</sub>-2.5-400 samples obtained after CaO<sub>2</sub> assisted calcination of the as-made organic-inorganic composite with a weight ratio (PEO-*b*-PS: In<sub>2</sub>O<sub>3</sub>) of 2.5 in air at 400 °C for 0.5 h (a), 1h (b), and 1.5h (c), respectively. The gradual increase of diffraction intensity indicates an ever-increasing degree of crystallization of In<sub>2</sub>O<sub>3</sub> with the prolonging calcination treatment time from 0.5 to 1.5 h.

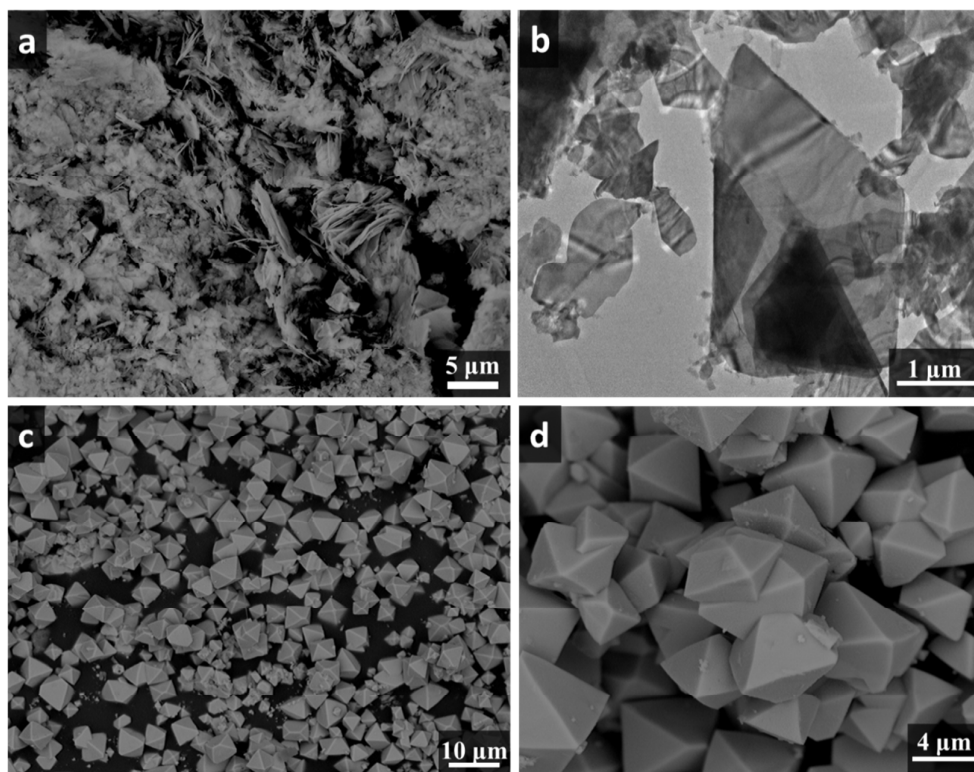


**Figure S4.** SEM (a, c, d) and TEM (b) images of the In<sub>2</sub>O<sub>3</sub> sample obtained by direct calcination of InCl<sub>3</sub> in air at 400 °C for 0.5h (a, b) and at 450 °C for 0.5h (c, d).

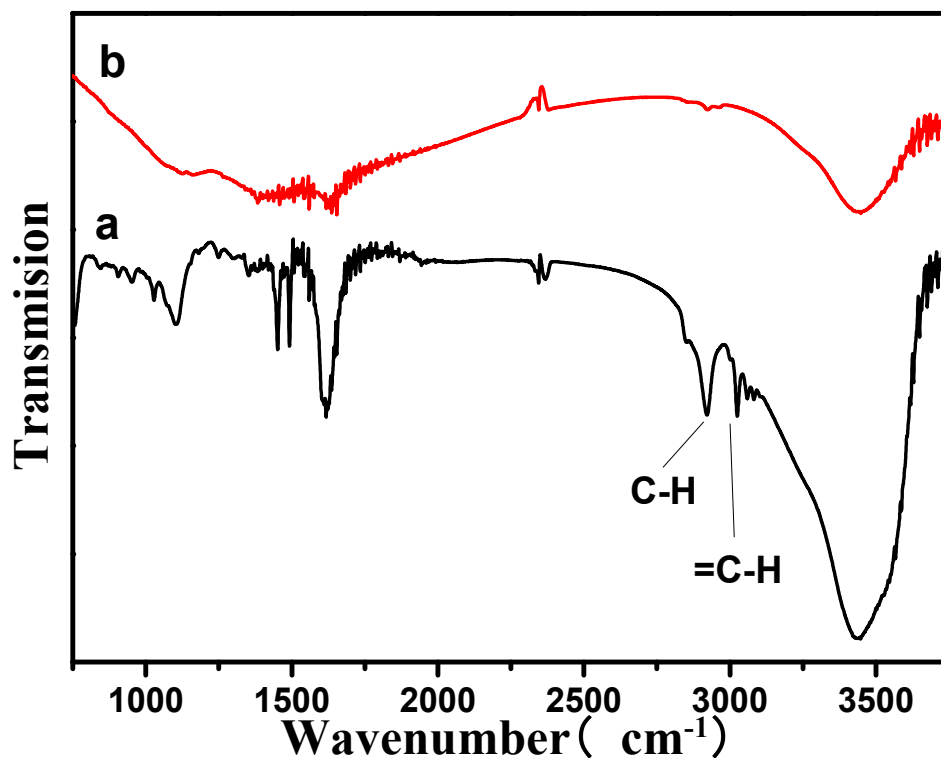


**Figure S5.** FTIR spectrum of (a) as-made PEO-*b*-PS/ $\text{In}_2\text{O}_3$  composite and (b) the mesoporous  $\text{In}_2\text{O}_3$  -2.5-400-0.5 obtained after calcination at 400 °C in air for 0.5h. Before calcination, typical absorption peaks at 2918  $\text{cm}^{-1}$  and 3024  $\text{cm}^{-1}$  can be clearly visible in the as-made PEO-*b*-PS/ $\text{In}_2\text{O}_3$  composite. While after calcination at 400 °C in air for 0.5h, all these peaks disappear, implying a complete removal of the PEO-*b*-PS copolymers.

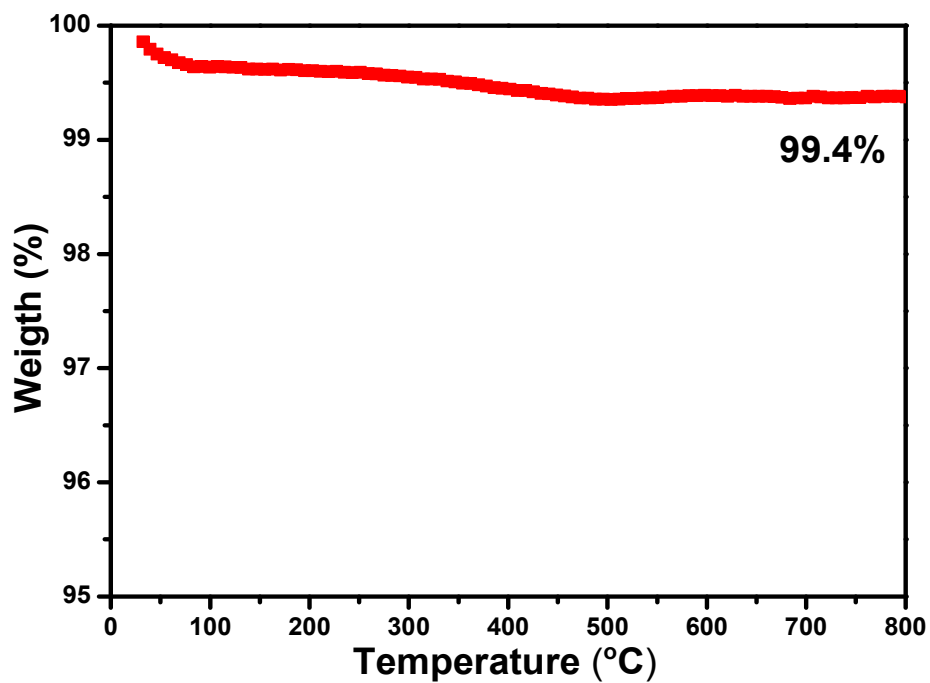


**Figure S6.** TG curves of the mesoporous  $\text{In}_2\text{O}_3$ -2.5-400-0.5 sample obtained after calcination at 400 °C in air for 0.5 h. It indicates a negligible weight loss of about 0.6% until 800 °C, confirming the complete removal of PEO-*b*-PS molecules after calcination at 400 °C in air with the assistance of  $\text{CaO}_2$ .

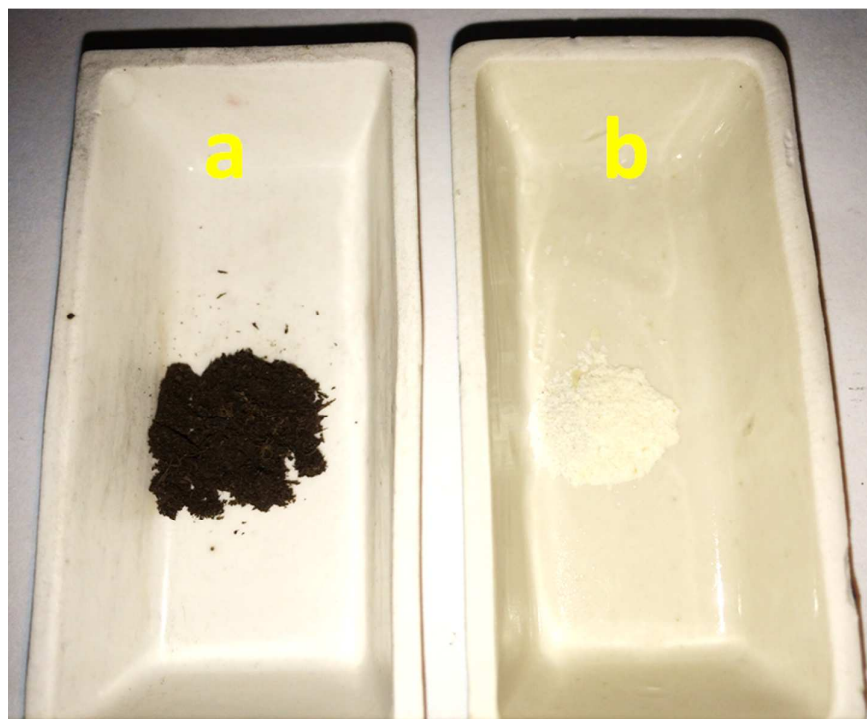


**Figure S7.** optical photographs of the mesoporous  $\text{In}_2\text{O}_3$  obtained after calcination in air at 400 °C for 0.5 h with the absence of  $\text{CaO}_2$  (a) and with the presence of  $\text{CaO}_2$  (b). It clearly indicates that without the use of  $\text{CaO}_2$ , the PEO-b-PS copolymers can be carbonized after quick calcination at 400 °C even in air due to the incomplete combustion, yielding a black sample. By contrast, with the presence of comburent  $\text{CaO}_2$ , the PEO-b-PS copolymer can be quickly decomposed, resulting in a light yellow powder sample.

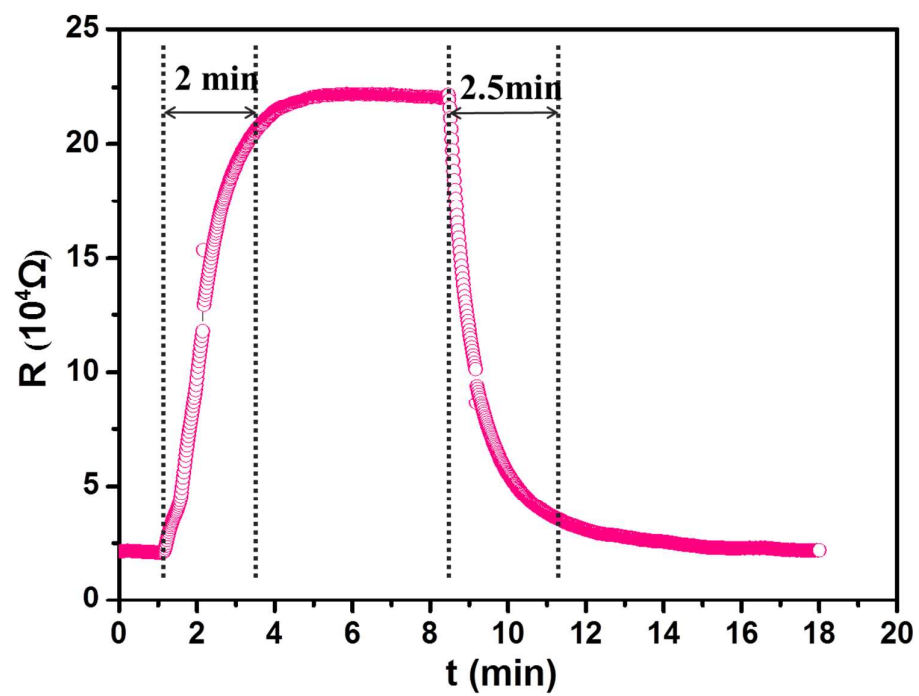


**Figure S8.** The response-recovery curve of the crystalline mesoporous indium oxides-based sensor to 250 *ppb* of  $\text{NO}_2$  at 150 °C.

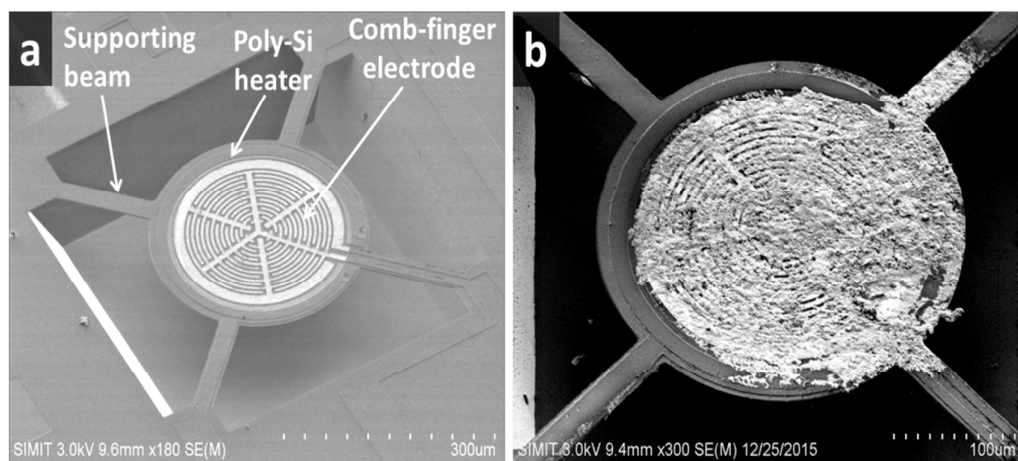


**Figure S9.** SEM images of the micro-hotplate chips before (a) and after depositing mesoporous  $\text{In}_2\text{O}_3$  (b).

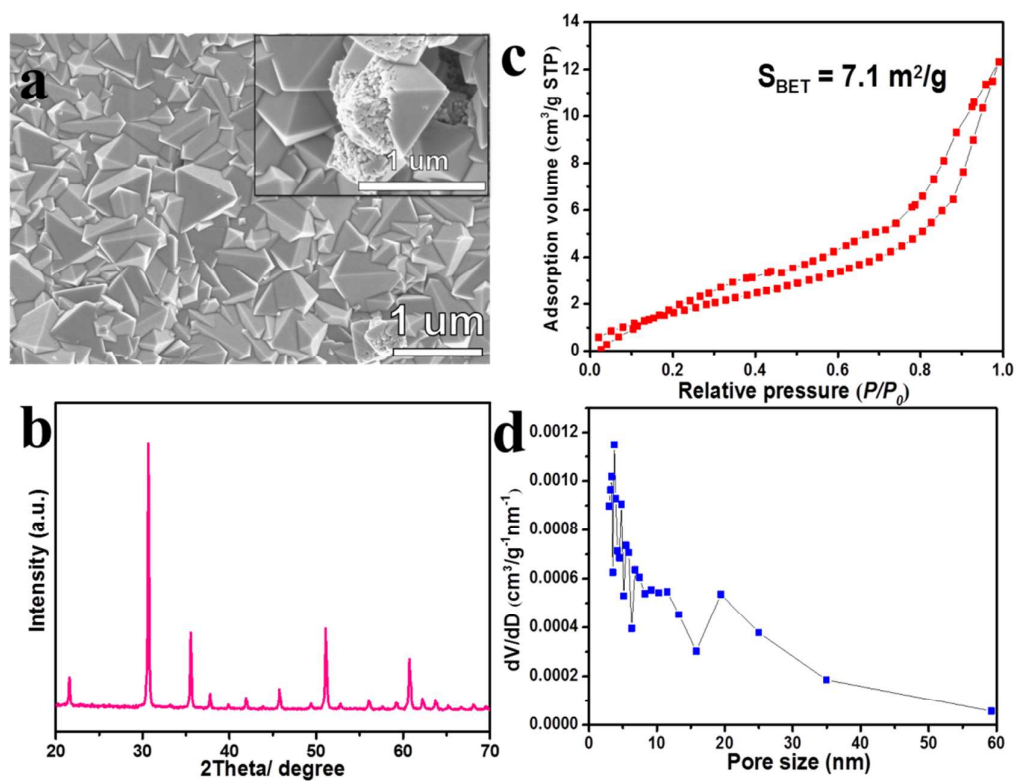


**Figure S10.** (a) SEM image, (b) XRD pattern, (c) the nitrogen adsorption-desorption isotherms and (d) the corresponding pore size distribution profile of the  $\text{In}_2\text{O}_3$ -2.5-450-1.0 sample.